OPEN ACCESS

International
Journal
Of Modern Engineering Research (IJMER)

Screening of Anti-Gastric Cancer Active Compounds and Potential Targets of *Pluchea indica* Based on Network Pharmacology and Molecular Simulation

HuixinTian[1], Hongyu Cao[1,2,3], Qian Tang[1,2], Lihao Wang[1]

[1]*College of Life and Health, Liaoning Key Laboratory of Bio-Organic Chemistry, Dalian University, Dalian, P.R. China.*

[2]*Dalian Institute of Marine Traditional Chinese Medicine, Dalian, P.R. China.*

[3]*State Key Laboratory for Quality Ensurance and Sustainable Use of Dao-di Herbs, Beijing, P.R. China.*

Corresponding Author: Hongyu Cao

ABSTRACT: *Combining network pharmacology and multi-dimensional molecular simulations, this work screened anti-gastric cancer bioactive ingredients and core targets of Pluchea indica, and analyzed ligand-protein binding profiles and dynamic stability. Shared targets of P. indica and gastric cancer were retrieved for PPI network, GO and KEGG enrichment analyses, demonstrating its multi-component, multi-target and multi-pathway anti-cancer mechanism. To avoid algorithmic bias, cross-validated molecular docking was performed using AutoDock and LibDock, and only high-affinity HRAS-ligand complexes were reserved. A 100 ns molecular dynamics simulation was implemented; RMSD, RMSF, intermolecular hydrogen bonds and Rg were measured to assess complex dynamic stability. Computational results indicated that P. indica suppresses gastric cancer via modulating tumor-related signaling pathways. Plucheoside D1 and D2 stably occupied the HRAS active pocket through hydrogen bonds and π-cation interactions, stabilizing the protein skeleton and restricting residue flexibility. Plucheoside D2 showed stronger binding capacity and sustained hydrogen bonding. In summary, the two monomers are promising HRAS-targeted candidates. Dual-software cross-verification improves simulation reliability and provides theoretical basis for exploring the anti-gastric cancer material basis of P. indica and developing HRAS-directed lead compounds.*

KEY WARDS: *Pluchea indica, Gastric cancer, Network pharmacology, Molecular docking, Molecular dynamics simulation*

Date of Submission: 19-08-2026 Date of acceptance: 31-08-2026

I. INTRODUCTION

Gastric cancer is a highly prevalent malignant tumor worldwide with persistently high morbidity and mortality rates, posing a severe threat to human health[1-2]. This tumor disease is characterized by high heterogeneity, with scarce precise therapeutic targets and an immature targeted therapy system in clinical practice. Chemotherapy and radiotherapy remain the dominant clinical treatment modalities. However, they are accompanied by obvious toxic side effects, interindividual therapeutic differences, and drug resistance after long-term administration. These drawbacks lead to poor prognosis, high recurrence rate and low long-term survival rate in patients, resulting in prominent limitations in clinical treatment[3-4]. In recent years, the discovery of low-toxicity and high-efficiency anti-tumor active substances from natural medicinal plants has become a hot spot in the research and development of new anti-cancer drugs[5-7]. Benefiting from the synergistic regulatory advantages of multi-component, multi-target and multi-pathway modes, traditional Chinese medicines possess great application potential in the research of tumor intervention[8].

Pluchea indica (L.) Less., a perennial shrub belonging to the genus *Pluchea* of the Asteraceae family, is the botanical source of Luanxi. Its dried stems, leaves and roots are used as a characteristic Lingnan medicinal and edible homologous herb, which is also known by aliases such as Yanxi, Wuxiangxiang and Gezashu[9]. It exhibits strong salt tolerance and belongs to mangrove-associated symbiotic plants. It is mainly distributed in coastal regions and offshore islands of South China, with its native range covering Asian areas including India, Myanmar, Indochina Peninsula and Malaysia. Meanwhile, it has been widely introduced to Pacific islands as an exotic species[10-11]. In China, Luanxi was first recorded in Lingnan Medicinal Herb Records, and it is also documented in multiple authoritative botanical and marine materia medica classics[12-13]. It is sweet in flavor

and slightly warm in nature, acting on the Stomach and Liver meridians. It can warm the middle energizer to dispel cold, invigorate the stomach to eliminate food stagnation, soften hard masses and dissipate stagnation, and is commonly used for the regulation of epigastric pain, abdominal distension caused by food retention and other related disorders. Locals in Lingnan often collect its fresh leaves to make herbal tea and Luanxi cakes, which can invigorate the spleen, warm the stomach, remove stagnant food and prevent epidemic diseases, with a long history of folk application[14]. Modern pharmacological studies have demonstrated that *Pluchea indica* (Luanxi) contains a variety of bioactive constituents, including sesquiterpenes, flavonoids, phenolic acids and sterols[15-16]. It possesses multiple pharmacological activities such as antioxidant[17-19], anti-inflammatory[20], antibacterial[21-24], lipid-regulating and hypoglycemic[25-27], wound healing-promoting[28], cell proliferation-inhibitory[29-30] and anti-tumor effects[31-33], showing great potential for medicinal development.

From the perspective of traditional Chinese medicine, the core pathogenesis of gastric cancer is the binding of blood stasis and toxin with accumulation stagnation in the stomach cavity. The effects of *Pluchea indica* in eliminating stagnation, dissipating masses and acting on the stomach meridian are highly consistent with this pathogenesis[34-36]. Furthermore, it has been proven to exert anti-tumor activity, indicating its potential value for the intervention of gastric cancer. However, there is still no systematic research focusing on the anti-gastric cancer mechanism of *Pluchea indica*, and its core active compounds and key therapeutic targets remain unclear. Accordingly, this study integrates multi-dimensional computational approaches including network pharmacology, molecular docking and molecular dynamics simulations to systematically dissect the synergistic characteristics of multi-component and multi-target effects of *Pluchea indica* against gastric cancer, providing fundamental theoretical support for subsequent experimental verification and the development of natural anti-gastric cancer drugs.

II. MATERIAL AND METHODS

2.1 Acquisition of Active Compounds and Corresponding Targets of Pluchea indica

Eleven major chemical constituents of *Pluchea indica* recorded in the monograph *Chemistry of Marine Chinese Materia Medica* were selected as research objects[37], namely plucheol A, plucheol B, plucheoside A, plucheoside B, plucheoside C, plucheoside D1, plucheoside D2, plucheoside D3, plucheoside E, pterocarptriol and tangshenoside II. The corresponding molecular structures of these compounds were downloaded from the PubChem database (https://pubchem.ncbi.nlm.nih.gov/). Target prediction of active compounds was performed using the SwissTargetPrediction database (http://www.swisstargetprediction.ch/) with the species set to *Homo sapiens*.

2.2 *Prediction of Disease Targets for Gastric Cancer*

Using "Gastric Cancer" as the keyword, gastric cancer-related targets were retrieved from five databases, including GeneCards (http://www.genecards.org/), DrugBank (https://go.drugbank.com/drugs/), OMIM (http://omim.org/), TTD (https://db.idrblab.net/ttd/) and ClinPGx (https://www.clinpgx.org/).

2.3 Screening of Overlapping Targets and Construction of PPI Network

The targets of active compounds from *Pluchea indica* and gastric cancer-related disease targets were intersected to obtain shared targets. The online tool Venny 2.1.0 (https://bioinfogp.cnb.csic.es/tools/venny/) was used for visualizing the intersection results. Subsequently, the overlapping targets were imported into the STRING database (https://string-db.org/) to construct a protein-protein interaction (PPI) network. The data exported from STRING were imported into Cytoscape 3.10.3 for network visualization and topological characteristic analysis. The CytoHubba plugin was applied to calculate network topological parameters, and core targets with high centrality were screened based on the ranking of Degree values.

2.4 GO and KEGG Enrichment Analysis

To clarify the biological functions and potential signaling pathways of overlapping targets, the Database for Annotation, Visualization and Integrated Discovery (DAVID, https://davidbioinformatics.nih.gov/) was used for gene functional annotation and enrichment analysis with the species set to Homo sapiens. The analytical items covered Gene Ontology (GO) functions including biological process (BP), molecular function (MF) and cellular component (CC), as well as Kyoto Encyclopedia of Genes and Genomes (KEGG) pathways. The online bioinformatics platform Bioinformatics (https://www.bioinformatics.com.cn/) was adopted to visualize and plot statistically significant enrichment results.

2.5 Molecular Docking

Standard molecular structures of active compounds were retrieved from the PubChem database, and the three-dimensional crystal structures of overlapping target proteins were downloaded from the RCSB PDB

database (https://www.rcsb.org/). Protein pretreatment was performed, including water molecule and native ligand removal, hydrogen atom addition, charge assignment based on the CHARMm force field, and repair of missing amino acid residues, so as to obtain receptor proteins available for docking. A dual docking strategy combining AutoDock and Discovery Studio LibDock was adopted to comprehensively evaluate the binding capacity between compounds and targets.

2.6 *Molecular Dynamics Simulation*

The screened core compound-target complexes were selected, and the optimal conformations obtained from molecular docking were taken as initial structures for molecular dynamics (MD) simulations. The simulation systems were constructed using GROMACS 2022.06 software. The AMBER03 force field and TIP3P water model were assigned to the complexes, and 0.15 M NaCl was added to maintain the physiological ionic environment of the system. Energy minimization, NVT equilibration at 310 K and NPT equilibration under 1 atm were carried out sequentially, followed by 100 ns MD simulations. Four indicators, including the root-mean-square deviation (RMSD) of the protein backbone, root-mean-square fluctuation (RMSF) of residues, ligand-protein hydrogen bond interactions, and radius of gyration (Rg) of the protein, were analyzed to comprehensively evaluate the system stability and molecular binding characteristics of the complexes.

III. RESULTS AND DISCUSSIONS

3.1 *Acquisition of Active Compounds and Corresponding Targets of Pluchea indica*

The chemical structures of the 11 active compounds are shown in (Fig. 1). Target prediction was performed via the SwissTargetPrediction database, yielding a total of 235 initial targets. After duplicate removal, 118 non-redundant potential targets of *Pluchea indica* were retained for subsequent network analysis.

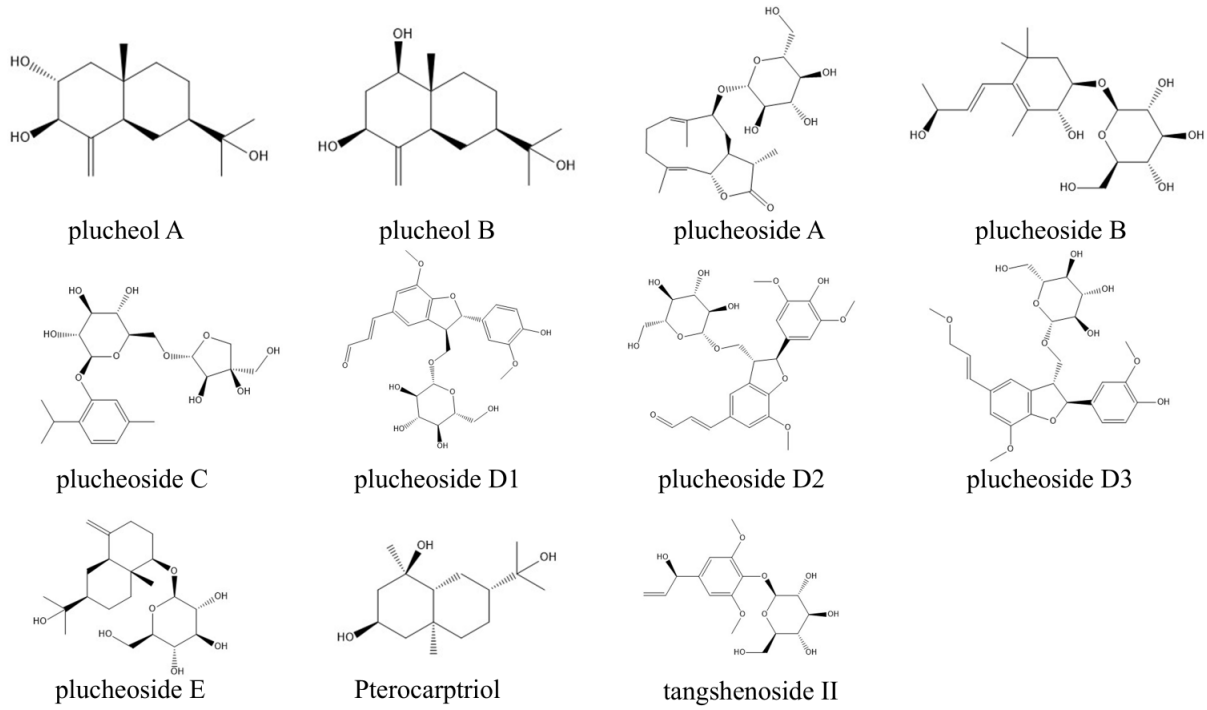

Figure 1: Structures of 11 Active Compounds of *Pluchea indica*

3.2 *Prediction of Disease Targets for Gastric Cancer*

Five disease databases were searched with the keyword "Gastric Cancer". A total of 764 targets with a relevance score higher than 25 were screened from GeneCards. Meanwhile, 170, 513, 2 and 2 targets were retrieved from DrugBank, OMIM, TTD and ClinPGx respectively. All collected targets were combined and deduplicated, and finally 1298 gastric cancer-related disease targets were obtained.

3.3 *Screening of Overlapping Targets and Construction of PPI Network*

After intersecting the targets of *Pluchea indica* active compounds and gastric cancer-related targets, a total of 25 overlapping targets were obtained (Fig. 2). These overlapping targets were imported into the STRING database with the species set as Homo sapiens, and the minimum interaction threshold was defined as medium confidence (>0.4), while other parameters remained at default values to construct the protein-protein

interaction (PPI) network (Fig. 3A). Cytoscape 3.10.3 was adopted for network visualization and topological analysis. The PPI network consisted of 25 nodes and 131 interaction edges (Fig. 3B), indicating tight interconnections among these targets. The Degree value of each node was applied to judge the centrality of targets in the network; a higher Degree value represented a stronger hub regulatory role of the target in the anti-gastric cancer network of *Pluchea indica*. Topological analysis revealed that the top 10 targets ranked by Degree were IL6, ESR1, STAT3, FGF2, PTGS2, HSP90AA1, IL2, HRAS, PIK3CA and JAK2.

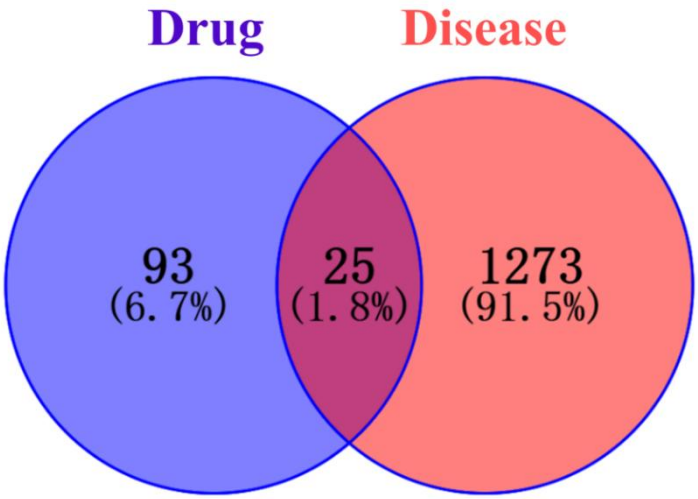

Figure 2: Venn Diagram of Potential Targets Shared between *Pluchea indica* and Gastric Cancer

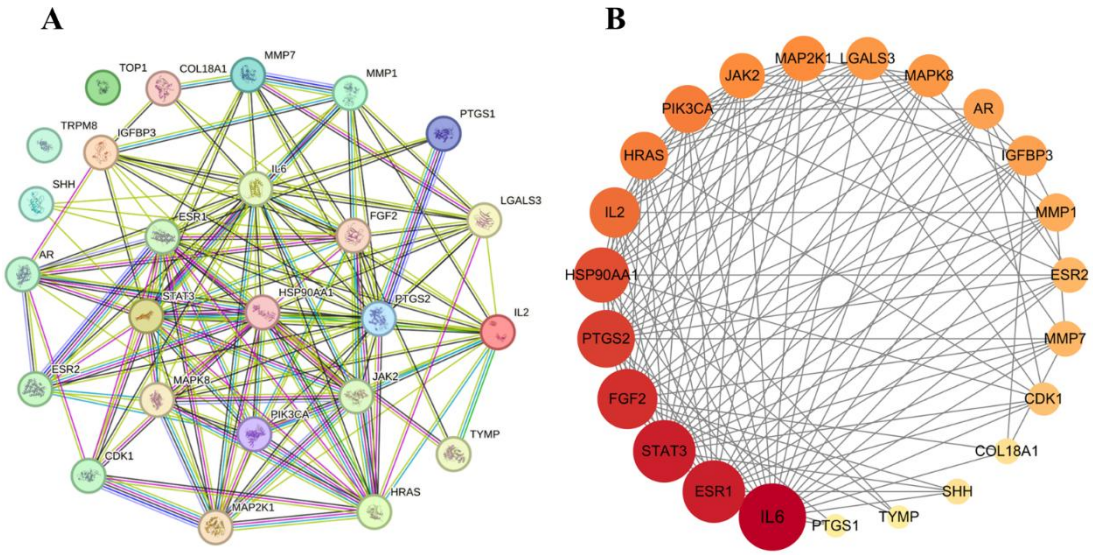

Figure 3: PPI Network of Overlapping Targets of *Pluchea indica* and Gastric Cancer
Note: A: Original PPI network from STRING; B: Hub target network ranked by Degree after Cytoscape topological analysis. Nodes with darker color and larger size possess higher Degree values.

3.4 *GO and KEGG Enrichment Analysis*

Gene Ontology (GO) functional enrichment classified target genes into three categories, namely biological process (BP), cellular component (CC) and molecular function (MF) (Fig. 4). In terms of biological processes, the target genes were significantly enriched in the regulation of gene expression, regulation of MAPK cascade, regulation of cell proliferation, negative regulation of apoptosis and other biological processes. Cellular components were mainly concentrated in the cell nucleus, cytoplasm, extracellular matrix and other regions. As for molecular functions, protein binding, serine/threonine kinase activity, enzyme binding and growth factor activity occupied the dominant positions. These results suggested that the active compounds of *Pluchea indica* exert anti-gastric cancer effects by regulating signal pathways related to gene transcription, cell proliferation and apoptosis.

To systematically dissect the potential signaling pathways underlying the anti-gastric cancer effect of *Pluchea indica*, KEGG pathway enrichment analysis was performed on overlapping target genes. A total of 107 signaling pathways were enriched, and the top 20 pathways with the smallest P-values were selected for visualization (Fig. 5). The target genes were significantly enriched in classic tumor-related pathways including pathways in cancer, PI3K-Akt, VEGF and FoxO signaling pathways. Meanwhile, several pathways governing tumor progression and therapeutic resistance were also enriched, such as EGFR tyrosine kinase inhibitor resistance and the AGE-RAGE signaling pathway. All the above pathways participate in the proliferation, invasion and signal transduction of gastric cancer cells, which verifies that *Pluchea indica* suppresses gastric cancer progression through synergistic regulation of multiple targets and multiple pathways.

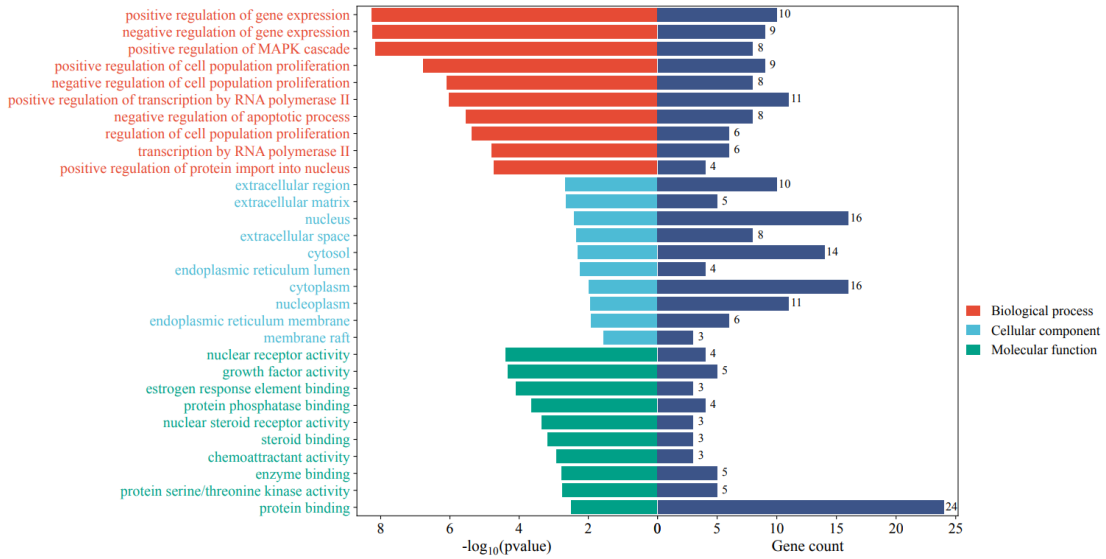

Figure 4: GO Enrichment Analysis of Overlapping Targets of *Pluchea indica* and Gastric Cancer

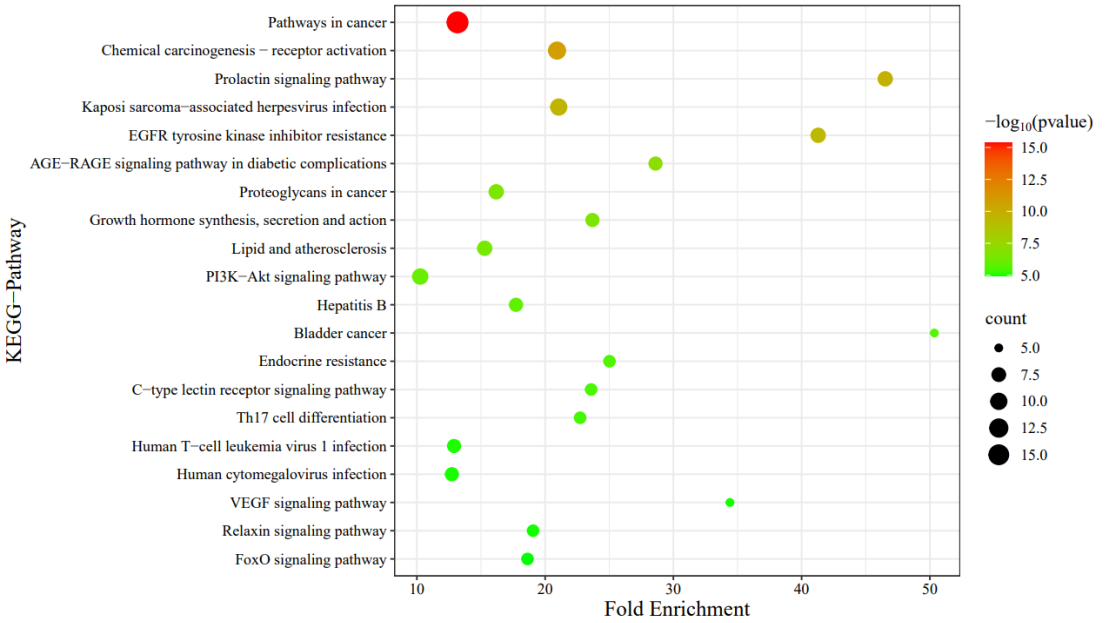

Figure 5: KEGG Pathway Enrichment Analysis of Overlapping Targets of *Pluchea indica* and Gastric Cancer

3.5 *Molecular Docking*

To verify the predictions of network pharmacology at the molecular structural level, active pocket prediction was performed on the proteins of the 25 overlapping targets. Since no valid binding pocket was

identified for VEGFA, systematic molecular docking was finally carried out between the remaining 24 target proteins and the 11 active compounds. Preliminary screening results from AutoDock revealed that the binding free energy of most compound-target pairs was lower than -7 kcal/mol, indicating generally stable binding potential between each compound and its corresponding target. The ligand conformation with the optimal binding energy for each target was extracted, and refined LibDock docking was implemented centered on the binding pocket; the corresponding results are presented in (Fig. 6). The LibDock scores varied widely, reflecting obvious differences in spatial complementarity and molecular interactions between distinct compounds and targets. Pairs without valid LibDock scores exhibited poor conformational matching and were excluded from subsequent analyses. Collectively, these findings confirm favorable structural affinity between partial active compounds of *Pluchea indica* and core targets, providing data support for screening highly reliable compound-target combinations.

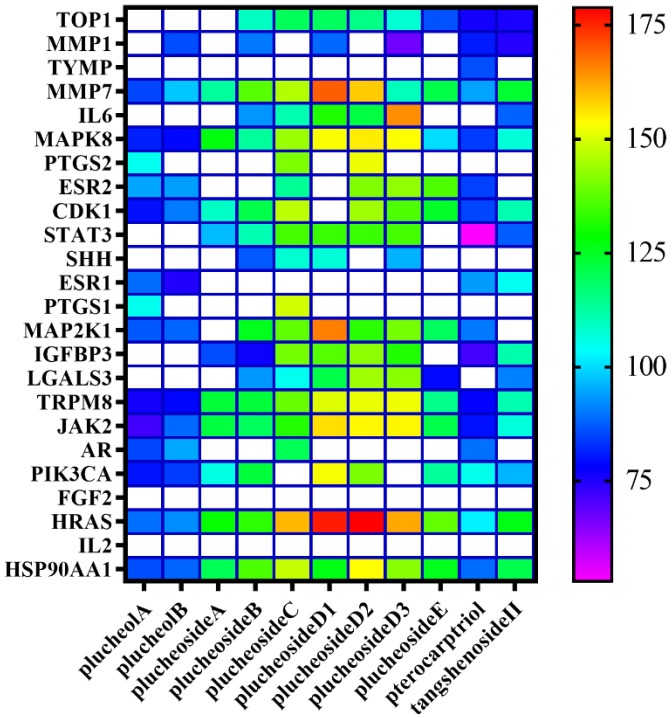

Figure 6: Heatmap of LibDock Scores for Active Compounds of *Pluchea indica* and Overlapping Gastric Cancer Targets

Note: The color gradient corresponds to LibDock scores. Purple indicates low scores, while red represents high scores. Blank cells stand for pairs without valid docking scores.

As observed from the LibDock heatmap, the docking scores of HRAS combined with plucheoside D1 and plucheoside D2 were significantly higher than those of other compound-target pairs, indicating outstanding binding affinity between the two compounds and HRAS. These two high-scoring complexes were selected to analyze their detailed molecular interactions (TableI, Fig. 7). The 3D structure of HRAS revealed that both plucheoside D1 and plucheoside D2 could stably embed into the active pocket of the protein. The enlarged view of the binding pocket demonstrated that the two ligands formed abundant hydrogen bonds and hydrophobic interactions with key amino acid residues of HRAS, and numerous hydrogen bond donors and acceptors were distributed at the binding interface. The 2D interaction diagram further confirmed that the two compounds established a stable binding network with HRAS through multiple non-covalent interactions. Both compounds bind to residue LYS117 via π-cation interactions. Specifically, plucheoside D2 simultaneously forms conventional hydrogen bonds with LYS117, while plucheoside D1 only exhibits a single π-cation interaction. In addition, both ligands are able to form conventional hydrogen bonds and carbon-hydrogen bonds with GLU31, ASP30, ASN116, SER17, THR35, THR58 and GLN61, as well as π-alkyl interactions with ALA18. The two compounds possess markedly different exclusive binding sites. Plucheoside D1 specifically binds to residues GLY12, SER145 and LYS147, whereas plucheoside D2 lacks the above intermolecular interactions and selectively binds to GLY13, ASP119 and ALA146 residues. In terms of overall binding mode, compared with

plucheoside D1, plucheoside D2 exerts two types of intermolecular forces at the LYS117 site, which endows it stronger transient binding affinity at the static docking level.

HRAS belongs to the small guanosine triphosphate (GTP)-binding Ras protein family, which represents one of the most thoroughly investigated signaling molecules in eukaryotic cells. *HRAS* dynamically switches between two conformations: the GTP-bound active state and the GDP-bound resting state, and it participates in regulating physiological processes including cell growth, differentiation, metabolism, survival and immune responses[38]. The Ras family consists of three homologous isoforms, namely *HRAS*, *KRAS* and *NRAS*. Although their protein structures are highly homologous, they differ in subcellular localization and regulatory functions. Oncogenic mutations in *HRAS* trigger persistent dysregulation of downstream signaling cascades and induce a variety of human malignant tumors, making *HRAS* a core research target in oncology. Accumulating evidence has verified that aberrant activation of *HRAS* is directly involved in the initiation and malignant progression of gastric cancer[39-42]. In this study, plucheoside D1 and plucheoside D2 were screened out via cross-validation using dual software for molecular docking. Both compounds exhibited excellent binding performance with HRAS under static conditions. Nevertheless, molecular docking only captures instantaneous static binding conformations and cannot evaluate the long-term stability of simulation systems. Therefore, 100 ns molecular dynamics (MD) simulations were further carried out to dynamically compare the conformational retention capacity of the two complexes.

Table I. **Docking Results of plucheoside D1/D2 and HRAS**

Compound Name	Target Name	AutoDock score	LibDock score
plucheoside D1	HRAS	-8.9 kcal/mol	175.972
plucheoside D2	HRAS	-8.4 kcal/mol	178.82

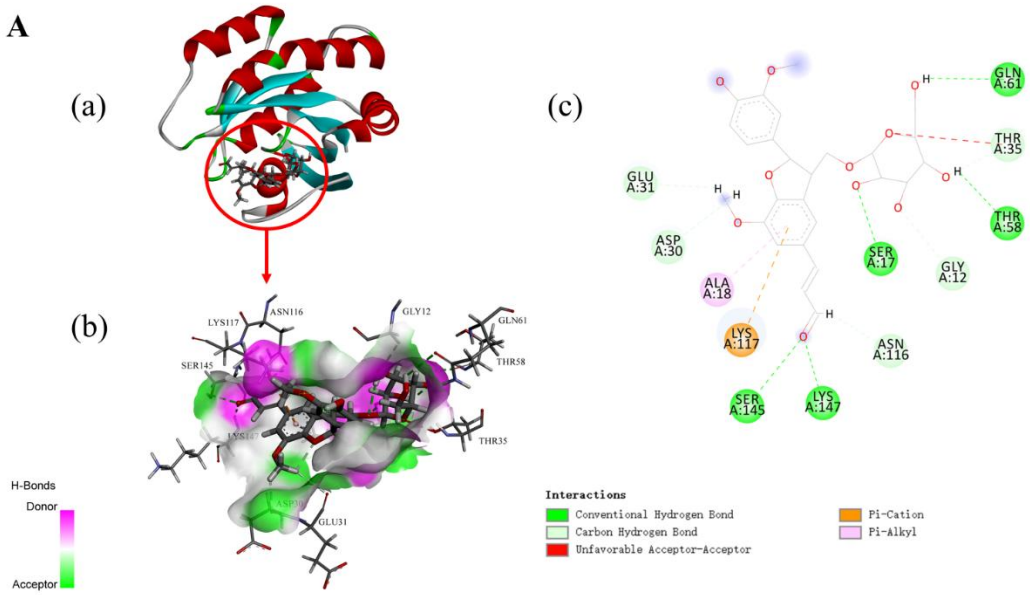

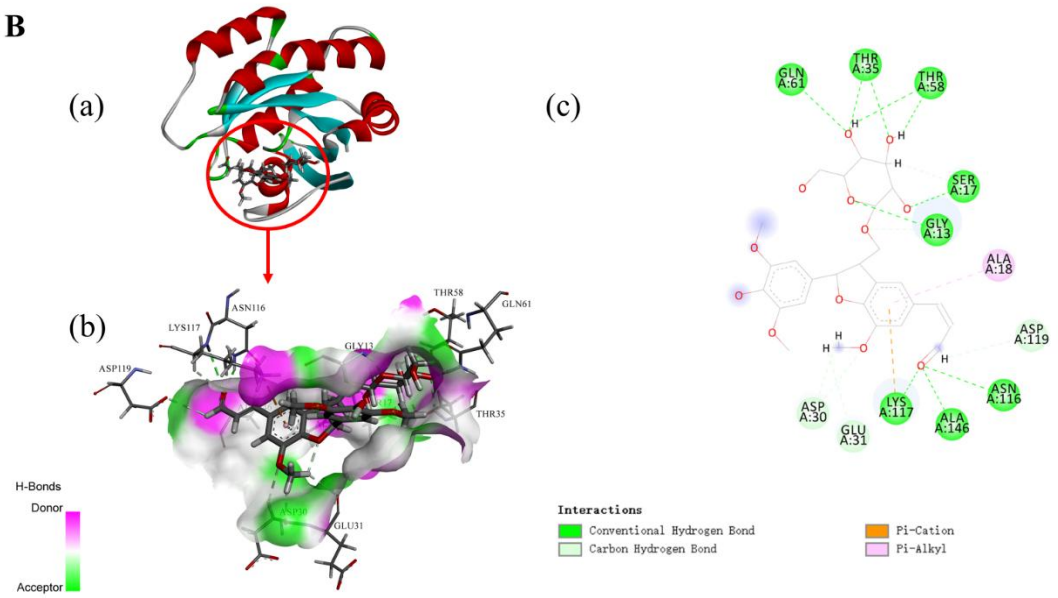

Figure 7: Docking Pattern Diagrams of plucheoside D1/D2 and HRAS

Note: A: HRAS-plucheoside D1 complex; B: HRAS-plucheoside D2 complex. (a) Overall binding position of the ligand; (b) Magnified view of the active pocket and surfaces of hydrogen bond donors and acceptors; (c) 2D diagram of non-covalent interactions between ligand and protein.

3.6 *Molecular Dynamics Simulation*

To dynamically evaluate the long-term binding stability of the two active compounds to HRAS, three simulation systems including free HRAS, HRAS-plucheoside D1 complex and HRAS-plucheoside D2 complex were constructed for 100 ns molecular dynamics simulations. Four parameters, namely RMSD, RMSF, the number of intermolecular hydrogen bonds and radius of gyration (Rg), were used to comprehensively assess the system stability, and the results are displayed in (Fig. 8).

The RMSD curve reflects the overall conformational fluctuation of the protein backbone. The baseline RMSD of free HRAS kept rising with the extension of simulation time and exhibited intense oscillation after equilibrium. The RMSD values of the two ligand-protein complexes were generally lower than those of free HRAS, and both remained below 0.3 nm, which met the judging criteria for stable protein complex systems[21]. Among them, the HRAS-plucheoside D2 system rapidly reached kinetic equilibrium after 60 ns with mild curve fluctuation. By contrast, the HRAS-plucheoside D1 system displayed a wider oscillation range after equilibrium, indicating inferior overall conformational stability compared with the HRAS-plucheoside D2 complex.

RMSF results revealed that both ligands could reduce the mobility flexibility of residues within the active pocket of HRAS. plucheoside D2 exerted a more remarkable inhibitory effect on the fluctuation of key amino acid residues in the binding region. In contrast, the C-terminal residues of the protein in the HRAS-plucheoside D1 system presented an obvious flexibility peak, demonstrating weaker conformational restriction capacity toward the active pocket compared with plucheoside D2.

Statistical analysis of intermolecular hydrogen bonds indicated that the HRAS-plucheoside D2 system stably maintained 2 to 8 intermolecular hydrogen bonds throughout the whole simulation process, forming a continuous and stable hydrogen bond network. In the HRAS-plucheoside D1 system, however, the number of hydrogen bonds gradually decreased as the simulation proceeded; the average number of hydrogen bonds dropped significantly after 60 ns, suggesting poor sustainability of intermolecular interactions.

The radius of gyration (Rg) was applied to evaluate the compaction degree of protein folding. The HRAS-plucheoside D2 system exhibited higher overall Rg values and remained stable within a fixed range in the later stage of simulation, meaning the protein could maintain a fully extended and functional conformation. In contrast, the Rg values of the HRAS-plucheoside D1 system fluctuated drastically, and the spatial compaction of the protein changed markedly over simulation time.

Comprehensive analysis of the four kinetic parameters demonstrated that both plucheoside D1 and plucheoside D2 could form stable binding systems with HRAS. Compared with plucheoside D1, plucheoside D2

performed better in stabilizing the protein backbone, restricting the flexibility of residues in the active pocket, and maintaining the intact spatial conformation of the protein. Meanwhile, it formed long-lasting hydrogen bond interactions, thus possessing stronger binding stability with HRAS. These findings were consistent with the results of previous static LibDock molecular docking scores and two-dimensional binding pattern analysis, which further verified that plucheoside D2 is the superior active ingredient targeting HRAS for the intervention of gastric cancer.

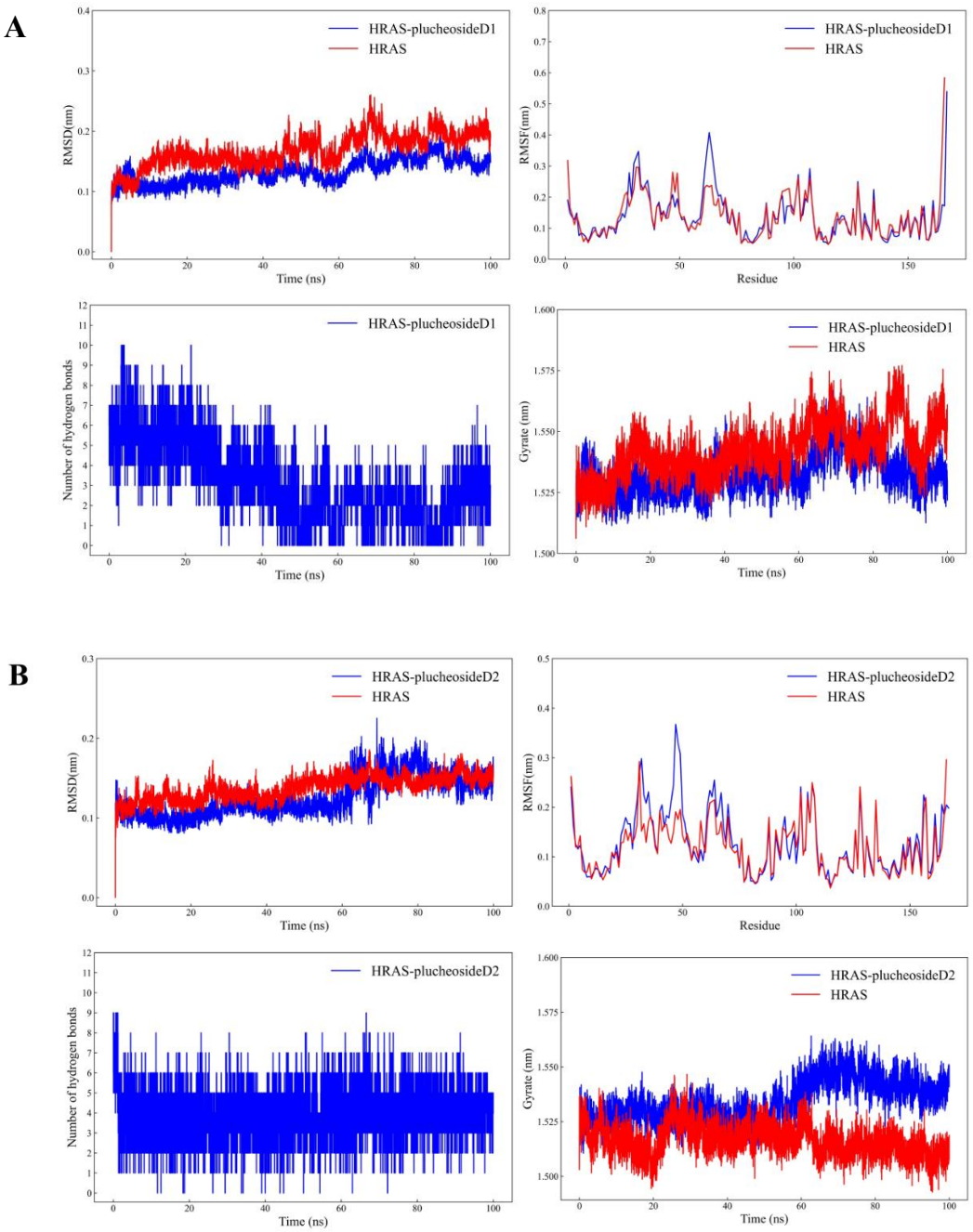

Figure 8: Results of 100 ns Molecular Dynamics Simulations of HRAS Complexes with plucheoside D1/D2 Note: A: HRAS-plucheoside D1 system; B: HRAS-plucheoside D2 system. Top left: RMSD curve; Top right: RMSF curve; Bottom left: Number of intermolecular hydrogen bonds; Bottom right: Rg curve. Red line: Free HRAS; Blue line: HRAS-ligand complex.

IV. CONCLUSIONS AND RECOMMENDATIONS

This study adopted network pharmacology, dual-software cross-validated molecular docking and 100 ns molecular dynamics simulations to screen anti-gastric cancer active constituents of *Pluchea indica* and characterize their binding behavior with therapeutic targets. Shared targets of *P. indica* and gastric cancer were retrieved, and PPI plus enrichment analyses demonstrated the herb acts against gastric cancer through multi-target, multi-pathway synergistic regulation. AutoDock and LibDock were jointly applied to eliminate single-algorithm bias, retaining only ligands with stable binding conformations in both tools. HRAS was screened as the core target, with plucheoside D1 and D2 identified as key bioactive monomers. Static docking validated both compounds anchored critical HRAS pocket residues via non-covalent interactions. Dynamics simulation further proved the two ligands stabilize HRAS conformation and suppress pocket residue flexibility; notably, the HRAS-plucheoside D2 complex showed better structural equilibrium, compact protein folding and sustained hydrogen-bond stability, delivering stronger target binding capacity.

In summary, this study constructed a progressive screening system consisting of broad-spectrum preliminary screening via network pharmacology, cross-verification through dual-program molecular docking, and dynamic validation by molecular dynamics simulations. The findings verified that plucheoside D1 and plucheoside D2 are superior active compounds derived from *P. indica* that have the potential to target HRAS and interfere with gastric cancer progression. All results of the present study are computational simulation predictions, which can provide theoretical references for exploring the material basis of *P. indica* against gastric cancer and developing small-molecule lead compounds targeting HRAS. Further in vitro and in vivo pharmacological experiments are still required to validate the actual anti-gastric cancer efficacy and molecular mechanisms of the two compounds.

REFERENCES

[1]. Bray, F., Laversanne, M., Sung, H., Ferlay, J., Siegel, R. L., Soerjomataram, I., & Jemal, A. (2024). Global cancer statistics 2022: GLOBOCAN estimates of incidence and mortality worldwide for 36 cancers in 185 countries. CA: a cancer journal for clinicians, 74(3), 229–263. https://doi.org/10.3322/caac.21834

[2]. Santos, M., Martins, D., & Mendes, F. (2025). Immunotherapy in gastric cancer-A systematic review. Oncology research, 33(2), 263–281. https://doi.org/10.32604/or.2024.052207

[3]. Joshi, S. S., & Badgwell, B. D. (2021). Current treatment and recent progress in gastric cancer. CA: a cancer journal for clinicians, 71(3), 264–279. https://doi.org/10.3322/caac.21657

[4]. Matheus, G. T. F. U., de Souza Wagner, P. H., Taumaturgo, J. A. C., Lam, S. J., & de Moraes, F. C. A. (2025). Preoperative Radiotherapy in Patients with Gastric and Gastro-Oesophageal Cancer: A Systematic Review and Meta-analysis. Journal of gastrointestinal cancer, 56(1), 84. https://doi.org/10.1007/s12029-025-01204-0

[5]. Newman, D. J., & Cragg, G. M. (2020). Natural Products as Sources of New Drugs over the Nearly Four Decades from 01/1981 to 09/2019. Journal of natural products, 83(3), 770–803. https://doi.org/10.1021/acs.jnatprod.9b01285

[6]. Chopra, B., & Dhingra, A. K. (2021). Natural products: A lead for drug discovery and development. Phytotherapy research: PTR, 35(9), 4660–4702. https://doi.org/10.1002/ptr.7099

[7]. Jia, Q., He, Q., Yao, L., Li, M., Lin, J., Tang, Z., Zhu, X., & Xiang, X. (2022). Utilization of Physiologically Based Pharmacokinetic Modeling in Pharmacokinetic Study of Natural Medicine: An Overview. Molecules (Basel, Switzerland), 27(24), 8670. https://doi.org/10.3390/molecules27248670

[8]. Rezvan, M., Hossini, S. E., Sarmast, K., &Khamesipour, F. (2025). The Efficiency of Plant Extracts in the Prevention of Gastric Cancer: A Systematic Review. Health science reports, 8(9), e71251. https://doi.org/10.1002/hsr2.71251

[9]. He, J. Q. (2011). *Alien plants in China*. Shanghai: Shanghai Science and Technology Press. (in Chinese)

[10]. Zhang, Y., Zhang, J., Yang, Y., & Liu, Q. (2017). Complete chloroplast genome of *Pluchea indica* (L.) Less. (Asteraceae) and its phylogenetic analysis. Mitochondrial DNA. Part B, Resources, 2(2), 918–919. https://doi.org/10.1080/23802359.2017.1413299

[11]. Ibrahim, S. R. M., Bagalagel, A. A., Diri, R. M., Noor, A. O., Bakhsh, H. T., & Mohamed, G. A. (2022). Phytoconstituents and Pharmacological Activities of Indian Camphorweed (*Pluchea indica*): A Multi-Potential Medicinal Plant of Nutritional and Ethnomedicinal Importance. Molecules (Basel, Switzerland), 27(8), 2383. https://doi.org/10.3390/molecules27082383

[12]. Xiao, B. D. (2009). *Records of Lingnan Medicinal Herbs*. Guangzhou: Guangdong Science and Technology Press. (in Chinese)

[13]. Xiao, G. L., Jiang, J. Y., Cheng, Q. Y., et al. (2023). Analysis of chemical constituents in leaves of *Pluchea indica* by UPLC-Q-TOF-MS/MS. *Journal of Instrumental Analysis, 42(*11), 1424–1433. https://doi.org/10.19969/j.fxcsxb.23062501. (in Chinese)

[14]. Cheng, Q. Y., Bi, X. L., Xin, X. F., et al. (2025). Comprehensive quality evaluation of *Pluchea indica* leaves from different habitats based on HPLC fingerprint combined with multivariate statistical analysis. *Chinese Journal of Medicinal Materials, 48*(11), 2804–2809. https://doi.org/10.13863/j.issn1001-4454.2025.11.023. (in Chinese)

[15]. Ruan, J., Yan, J., Zheng, D., Sun, F., Wang, J., Han, L., Zhang, Y., & Wang, T. (2019). Comprehensive Chemical Profiling in the Ethanol Extract of *Pluchea indica* Aerial Parts by Liquid Chromatography/Mass Spectrometry Analysis of Its Silica Gel Column Chromatography Fractions. Molecules (Basel, Switzerland), 24(15), 2784. https://doi.org/10.3390/molecules24152784

[16]. Ruan, J., Li, Z., Yan, J., Huang, P., Yu, H., Han, L., Zhang, Y., & Wang, T. (2018). Bioactive Constituents from the Aerial Parts of *Pluchea indica* Less. Molecules (Basel, Switzerland), 23(9), 2104. https://doi.org/10.3390/molecules23092104

[17]. Liao, R. Q., Su, B. W., Gong, B., et al. (2017). Extraction technology and antioxidant activity of flavonoids from leaves of *Pluchea indica*. *Journal of Qinzhou University, 32*(5), 1–7. (in Chinese)

[18]. Sirichaiwetchakoon, K., Lowe, G. M., &Eumkeb, G. (2020). The Free Radical Scavenging and Anti-Isolated Human LDL Oxidation Activities of *Pluchea indica* (L.) Less. Tea Compared to Green Tea (Camellia sinensis). BioMed research international, 2020, 4183643. https://doi.org/10.1155/2020/4183643

[19]. Nopparat, J., Nualla-Ong, A., &Phongdara, A. (2020). Treatment with *Pluchea indica* (L.) Less. leaf ethanol extract alleviates liver injury in multiple low-dose streptozotocin-induced diabetic BALB/c mice. Experimental and therapeutic medicine, 20(2), 1385‑1396. https://doi.org/10.3892/etm.2020.8877

[20]. Buapool, D., Mongkol, N., Chantimal, J., Roytrakul, S., Srisook, E., &Srisook, K. (2013). Molecular mechanism of anti-inflammatory activity of *Pluchea indica* leaves in macrophages RAW 264.7 and its action in animal models ofinflammation. Journal of ethnopharmacology, 146(2), 495–504. https://doi.org/10.1016/j.jep.2013.01.014

[21]. Wahyuni, D. K., Junairiah, J., Rosyanti, C., Kharisma, V. D., Syukriya, A. J., Rahmawati, C. T., Purkan, P., Subramaniam, S., Prasongsuk, S., &Purnobasuki, H. (2024). Computational and in vitro analyses of the antibacterial effect of the ethanolic extract of *Pluchea indica* L. leaves. Biomedical reports, 21(4), 137. https://doi.org/10.3892/br.2024.1825

[22]. Demolsky, W. L., Sugiaman, V. K., & Pranata, N. (2022). Antifungal Activity of Beluntas "Indian Camphorweed" (*Pluchea indica*) Ethanol Extract on Candida albicans In Vitro Using Different Solvent Concentrations. European journal of dentistry, 16(3), 637–642. https://doi.org/10.1055/s-0041-1736591

[23]. Prasasty, V. D., Cindana, S., Ivan, F. X., Zahroh, H., & Sinaga, E. (2020). Structure-based discovery of novel inhibitors of Mycobacterium tuberculosis CYP121 from Indonesian natural products. Computational biology and chemistry, 85, 107205. https://doi.org/10.1016/j.compbiolchem.2020.107205

[24]. Hikmawanti, N. P. E., Saputri, F. C., Yanuar, A., Jantan, I., Ningrum, R. A., &Mun'im, A. (2024). Insights into the anti-infective effects of *Pluchea indica* (L.) Less and its bioactive metabolites against various bacteria, fungi, viruses, and parasites. Journal of ethnopharmacology, 320, 117387. https://doi.org/10.1016/j.jep.2023.117387

[25]. Singdam, P., Naowaboot, J., Senggunprai, L., Boonloh, K., &Pannangpetch, P. (2022). *Pluchea indica* Leaf Extract Alleviates Dyslipidemia and Hepatic Steatosis by Modifying the Expression of Lipid Metabolism-Related Genes in Rats Fed a High Fat-High Fructose Diet. Preventive nutrition and food science, 27(4), 384–398. https://doi.org/10.3746/pnf.2022.27.4.384

[26]. Nopparat, J., Nualla-Ong, A., &Phongdara, A. (2019). Ethanolic extracts of *Pluchea indica* (L.) leaf pretreatment attenuates cytokine-induced β-cell apoptosis in multiple low-dose streptozotocin-induced diabetic mice. PloS one, 14(2), e0212133. https://doi.org/10.1371/journal.pone.0212133

[27]. Sirichaiwetchakoon, K., Lowe, G. M., Kupittayanant, S., Churproong, S., &Eumkeb, G. (2020). *Pluchea indica* (L.) Less. Tea Ameliorates Hyperglycemia, Dyslipidemia, and Obesity in High Fat Diet-Fed Mice. Evidence-based complementary and alternative medicine :eCAM, 2020, 8746137. https://doi.org/10.1155/2020/8746137

[28]. Buranasukhon, W., Athikomkulchai, S., Tadtong, S., &Chittasupho, C. (2017). Wound healing activity of *Pluchea indica* leaf extract in oral mucosal cell line and oral spray formulation containing nanoparticles of the extract. Pharmaceutical biology, 55(1), 1767–1774. https://doi.org/10.1080/13880209.2017.1326511

[29]. Kanphet, Y., Uttarawichien, T., Vongsak, B., Boonsom, T., Nalinratana, N., Sivaji, S., Towiwat, P., &Sukrong, S. (2025). Standardized *Pluchea Indica* Leaf Extract Exhibited Antiproliferative Activity Against TGF-β-induced Prostate Stromal Cells (WPMY-1) Through G 1 Phase Cell Cycle Arrest via SMAD2/3 and ERK1/2 Signaling Pathways. In vivo (Athens, Greece), 39(2), 778–794. https://doi.org/10.21873/invivo.13882

[30]. Cho, C. L., Lee, Y. Z., Tseng, C. N., Cho, J., Cheng, Y. B., Wang, K. W., Chen, H. J., Chiou, S. J., Chou, C. H., & Hong, Y. R. (2017). Hexane fraction of *Pluchea indica* root extract inhibits proliferation and induces autophagy in human glioblastoma cells. Biomedical reports, 7(5), 416–422. https://doi.org/10.3892/br.2017.979

[31]. Aishah Baharuddin, S., Nadiah Abd Karim Shah, N., Saiful Yazan, L., Abd Rashed, A., Kadota, K., Al-Awaadh, A. M., & Aniza Yusof, Y. (2023). Optimization of *Pluchea indica* (L.) leaf extract using ultrasound-assisted extraction and its cytotoxicity on the HT-29 colorectal cancer cell line. Ultrasonics sonochemistry, 101, 106702. https://doi.org/10.1016/j.ultsonch.2023.106702

[32]. Kao, C. L., Cho, J., Lee, Y. Z., Cheng, Y. B., Chien, C. Y., Hwang, C. F., Hong, Y. R., Tseng, C. N., & Cho, C. L. (2015). Ethanolic Extracts of *Pluchea indica* Induce Apoptosis and Antiproliferation Effects in Human Nasopharyngeal Carcinoma Cells. Molecules (Basel, Switzerland), 20(6), 11508–11523. https://doi.org/10.3390/molecules200611508

[33]. Trang, V. M., Son, N. T., Pham, T. V., & Giang, P. M. (2024). Essential Oils from the Leaves and Stem Barks of *Pluchea Indica* (L.) Less.: Chemical Analysis, Cytotoxicity, Anti-inflammation, Antimicrobial Activity, Molecular Docking, and ADMET Profiling. Chemistry & biodiversity, 21(12), e202401785. https://doi.org/10.1002/cbdv.202401785

[34]. Ke, J., Meng, C. C., & Chang, S. (2026). Exploration of Chang Qing's experience in treating gastric cancer with pathogen-eliminating and tumor-attacking herbs.*Zhejiang Journal of Traditional Chinese Medicine, 61*(7), 577–578. https://doi.org/10.13633/j.cnki.zjtcm.2026.07.003. (in Chinese)

[35]. Liu, Y. Y., Qu, Y. G., Liu, W. D., et al. (2025). Discussion on the pathogenesis of intermingled stasis, toxin and stagnation in gastric cancer based on "spleen stagnation leading to liver depression". *Liaoning Journal of Traditional Chinese Medicine, 52*(4), 55–58. https://doi.org/10.13192/j.issn.1000-1719.2025.04.015. (in Chinese)

[36]. Liu, Y. Y., Zhao, Z. Q., Liang, W. Y., et al. (2023). Connotation of pathogenesis evolution of intermingled blood stasis and toxin in gastric cancer from the perspective of "inflammation-carcinoma transition". *China Journal of Traditional Chinese Medicine and Pharmacy, 38*(6), 2518–2521. (in Chinese)

[37]. Hou, X. T., & Deng, J. G. (2018). *Chemistry of Marine Chinese Materia Medica*. Nanning: Guangxi Science and Technology Press. (in Chinese)

[38]. Husein, A., Jamal, A., Ali, R., Kamal, M. A., Alqurashi, Y. E., Nasim, A., Hussain, S. A., &Hattiwale, H. M. (2026). Ras signalling in infectious disease pathology: Mechanisms, tissue damage, and clinical implications. Pathology, research and practice, 286, 156609. Advance online publication. https://doi.org/10.1016/j.prp.2026.156609

[39]. Zhou, F., Zhu, C., Yuan, W., Peng, W., Xu, Q., Yang, H., Cao, R., Wang, B., Wang, M., & Xu, H. (2026). Asiatic Acid Ameliorates MNNG-Induced Chronic Atrophic Gastritis by Inhibiting the Activation of the HRAS/PI3K/AKT/GSK3β Signaling Axis. Phytotherapy research: PTR, 40(5), 2210–2229. https://doi.org/10.1002/ptr.70265

[40]. Yermekova, S., Orazgaliyeva, M., Goncharova, T., Rakhimbekova, F., Kaidarova, D., &Shatkovskaya, O. (2023). Characteristic Mutational Damages in Gastric and Colorectal Adenocarcinomas. Asian Pacific journal of cancer prevention: APJCP, 24(11), 3939–3947. https://doi.org/10.31557/APJCP.2023.24.11.3939

[41]. Wang, Y., Chu, F., Lin, J., Li, Y., Johnson, N., Zhang, J., Gai, C., Su, Z., Cheng, H., Wang, L., & Ding, X. (2021). Erianin, the main active ingredient of Dendrobium chrysotoxum Lindl, inhibits precancerous lesions of gastric cancer (PLGC) through suppression of the HRAS-PI3K-AKT signaling pathway as revealed by network pharmacology and in vitro experimental verification. Journal of ethnopharmacology, 279, 114399. https://doi.org/10.1016/j.jep.2021.114399

[42]. Zhang, H., Zhuo, H., Hou, J., & Cai, J. (2023). Machine learning models predict the mTOR signal pathway-related signature in the gastric cancer involving 2063 samples of 7 centers. Aging, 15(13), 6152–6162. https://doi.org/10.18632/aging.204817